

Chapter 6

Microtoroid reflow and measurement in vacuum

6.1 Introduction

The most commonly quoted specification of microcavities is quality factor, indeed it is now built into the name given to ultra-high Q (UHQ) microtoroids. Microtoroids have already leveraged their high Q to form single frequency lasers, a high resolution optical coupler, an efficient photon router and biological sensors [20, 19, 107, 30, 31]. All of these applications were made possible by the narrow linewidth of microtoroids modes.

The ultimate limit of microcavity Q , in microtoroids or microspheres for example, has been investigated theoretically and experimentally [6, 7, 108]. The theoretical upper limit on Q for millimeter sized fused silica microspheres is argued to be 1×10^{12} [108], an enormous figure that corresponds to a average photon propagation length of more than 200 km, or 40 million round trips. However, the highest Q measured to date in any silica microcavity is slightly less than 1×10^{10} for a microsphere. This discrepancy indicates that one or more sources of loss in microcavities is higher than predicted. The various sources of loss in optical microcavities will be given in Section 6.2.

Like microspheres, microtoroids have yet to reach their theoretical maximum quality factors. The highest Q measured until now in microtoroids is 4×10^8 [12], lower than microspheres. The lower Q in microtoroids may be partially explained by the higher mode confinement (in the azimuthal direction), which exposes higher field intensities of the cavity mode to surface imperfections and contaminants. Silica microtoroids have become the preferred microcavity for advanced experiments because they are easier to fabricate in large quantities on chip, have planar geometry, and have significantly lower mode volume than silica microspheres. Therefore, many applications will benefit from higher Q microtoroids, if the existing sources of loss may be reduced.

The author has directed novel research into increasing the Q of microtoroids by designing, building, and demonstrating a laser reflow and toroid measurement system in vacuum. Record high Q is expected in a water- and dust-free vacuum environment.

6.2 Sources of loss in microtoroids

In order to increase toroid Q to a record level, the reasons for finite Q must first be understood. Loss in microcavity resonators is caused by numerous sources, whose contributions can be quantified by attenuation coefficients (α_i), and corresponding quality factor Q_i . The relationship is defined as $Q_i = \frac{2\pi n}{\alpha_i \lambda}$. The total quality factor in UHQ microtoroid resonators can be expressed in terms of distinct components for each source of loss, as long as each loss factor is small over one cavity round trip [69].

$$Q_{tot}^{-1} = Q_{mat}^{-1} + Q_{WGM}^{-1} + Q_{ss}^{-1} + Q_{cont}^{-1} + Q_{water}^{-1} + Q_{ext}^{-1} \quad (6.1)$$

The major components of whispering-gallery resonator loss listed above are by no means a complete list, other loss factors may exist and can be accounted for easily. But, the major contributions to total Q include: the intrinsic loss of silica due to absorption and Rayleigh scattering (Q_{mat}), radiation loss of the WGM due to photon tunneling (Q_{WGM}), silica roughness induced surface scattering (Q_{ss}), absorption caused by surface contamination (Q_{cont}), absorption caused by OH groups or water molecules adsorbed into the silica toroid or attached to the surface, and external loss caused by useful taper coupling (Q_{ext}).

6.2.1 Intrinsic loss

Silica has a large transparency window including the visible and near infrared (NIR) wavelengths, making it the ideal dielectric medium for UHQ microcavity resonators. Silica has maximum transmission at 1550 nm, the communications band where the majority of optical information is carried around the world. The intrinsic attenuation factor of silica at 1550 nm is $\alpha_{mat} = 0.2 \text{ dB/km}$, which accounts for intrinsic absorption loss and Rayleigh scattering in silica.

Rayleigh scattering is the elastic scattering of light by particles or refractive index variations smaller than the wavelength of light. Normally, Rayleigh scattering losses calculated for plane waves in infinite media is applied without modification to curved microcavities. Gorodetsky deduced that mode confinement in microcavities can actually reduce Rayleigh scattering [108]. But, for the calculations in this chapter, the simple bulk intrinsic loss of silica is assumed for ease of calculation. Therefore, the intrinsic quality factor of silica is 3×10^{10} according to the expression given above. Since the highest Q recorded for a microtoroid is 4×10^8 , then the intrinsic loss in silica is not currently the limiting factor.

6.2.2 Whispering gallery loss

In whispering-gallery optical resonators, the optical modes are confined by continuous total internal reflection (TIR) at the silica-air interface. For infinite planar structures, light reflected at an angle below the TIR critical angle will be perfectly reflected assuming there are no absorption losses. But,

TIR on a curved interface like a microtoroid is not perfect, and a fraction of the circulating power leaks out as a transmitted wave [109]. Intuitively, a fraction of the circulating photons will strike the silica-air boundary at angles higher than the critical angle and escape. The fraction of photons that are able to tunnel out of the bound state of the WGM is dependent on the cavity radius as expected. FEM simulations of the microtoroid by Sean Spillane show that WGM loss decreases exponentially as a function of the toroid major radius. The WGM limited Q (Q_{WGM}) is greater than 10^{12} for toroids with major diameters (D) of 30 μm or larger and minor diameters (d) greater than 3 μm . Therefore, microtoroids with dimensions exceeding these figures are not limited by WGM loss, and the current limitation to Q in microtoroids must lie elsewhere.

6.2.3 External sources of loss

The two main sources of external loss in microtoroids are the fiber taper coupling and any contaminants that reside on the surface of the toroid. To analyze the effect of taper loading on cavity Q , first the basic properties of optical transfer between the taper and toroid must be discussed [69]. The transmission of the fiber taper can be written as

$$T \equiv \left(\frac{1 - K}{1 + K} \right)^2 \quad (6.2)$$

where K is the coupling factor defined as $K = \kappa_0^2/\sigma_0^2$ [13]. The coupling factor is the dimensionless ratio of the coupling coefficient (κ_0^2) and the intrinsic loss (σ_0^2).

Fiber taper coupling to a microtoroid can be separated into three regimes. Starting with a large gap between the toroid and taper, in the under coupled regime, the total Q of the toroid is dominated by the intrinsic loss ($K < 1$). When the toroid and taper are critically coupled, the coupling and intrinsic loss coefficients are identical ($K = 1$), and the transmission is zero due to destructive interference of the optical wave traveling down the fiber and the optical field inside the toroid, which is π out of phase. Microcavity lasers are typically operated close to critical coupling, where the stored energy inside the microtoroid is maximum, hence giving the highest pump absorption in the laser cavity. In the over coupled regime, waveguide coupling dominates the total Q ($K > 1$), and the taper is located even closer to the toroid.

The relationship between the total Q and the coupling (κ_0) and intrinsic (σ_0) loss components is:

$$Q_{tot} = \frac{2\pi c}{\lambda(\kappa_0^2 + \sigma_0^2)} \quad (6.3)$$

At critical coupling, $\kappa_0^2 = \sigma_0^2$, the quality factor is exactly half of its intrinsic value. This simple relationship between a measurement of Q at critical coupling and intrinsic Q is valid if the intermodal coupling caused by scattering is weak. Alternatively, the expression for calculating intrinsic Q at critical coupling in the presence of mode splitting was given in Equation (2.15) in **Chapter 2**.

The cavity loading effect on microtoroid Q is unavoidable if the cavity is to be used for any experiment. Therefore, the quantifiable reduction in Q at critical coupling as described above will be accounted for. In short, cavity loss due to taper coupling is not a concern for this research.

All other sources of external loss in microtoroids are grouped together as contamination. Some examples include dust from the air (e.g., human skin cells), silicon particles that are sputtered onto the microtoroid during laser reflow, and photoresist left behind during fabrication. These contaminants can be reduced or eliminated with clean fabrication techniques, proper wafer handling, storage of resonators in a clean nitrogen purged environment, laser reflow with appropriate power levels, and finally by protecting the microtoroids during experiment. The vacuum chamber built for this research project will help clean the toroids before reflow, and maintain their pristine quality during testing. But, the laser reflow in vacuum system is designed to reduce the effect of the most likely source for Q limitation in toroids, common water.

6.3 Microtoroid loss caused by water

Water is a key precursor present during wet-deposition of the thermal oxide layer that is processed into silica microtoroids. Although the thermal oxide layer is annealed at high temperature, residual OH ions can remain and cause significant loss in microtoroids. Also, water adsorbs onto the surface of the toroid in one or more monolayers of liquid H_2O if there is any water vapor present in the air. Since normal air has 30% relative humidity, water adsorption onto microtoroids tested in air is unavoidable. Near infrared light excites vibration of the rotational symmetry of the OH group in water or any chemically fashioned OH groups inside the amorphous silica. The attenuation coefficient of water at 1550 nm is $\alpha_{water} = 2.2 \times 10^3 \text{ m}^{-1}$ [22]. A microtoroid immersed completely in water will have lower Q for this reason, as discussed in **Chapter 4**.

The possibility of quality factor reduction caused by water has been considered in microspheres and microtoroids. In a manuscript that explores the limits of ultimate Q in microspheres, Gorodetsky demonstrates that water adsorption onto the surface of a 750 μm diameter microsphere causes a reduction in cavity Q [6]. Immediately after the microsphere is fabricated by flame, he observed a fast decrease of the cavity lifetime within two minutes. This behavior is consistent with the process of chemical formation of water monolayers on the surface of hydrophilic surfaces like silica [110]. The intrinsic Q of the microsphere drops from 8×10^9 to 1×10^9 within an hour. The initial microsphere Q is partially recovered by baking the microsphere at 400°C, giving strong evidence that water adsorption onto the microsphere surface is the source of limitation for maximum Q in microcavities. Theoretically, if the surface-tension induced reflow and testing could be performed in a perfectly dry environment, then the Q would not suffer due to water absorption. Here lies the exact aim of the research documented in this chapter – to reduce or remove the effect of water in microtoroids for

exploration of ultimate Q .

The interaction between water and microtoroid cavities was also studied by Rokhsari and Spillane [111]. The thermal bistability effect was applied for loss characterization of microtoroids, and showed that surface water causes heating of the toroid, and subsequently shifting of the cavity resonance. A FEM simulation was developed for studying the effect of water adsorbed on the surface of a microtoroid. The simulation added, to the surface of the silica microtoroid, a thin dielectric shell with the thickness of a monolayer of water and the attenuation coefficient of water. The maximum Q factor for a microtoroid with such a monolayer of water is predicted to be 7×10^8 , close to the highest Q value recorded for microtoroids.

The body of work presented above suggests that absorption loss caused by water may be the limiting factor to ultimate Q in current microtoroid research. If vacuum reflow and toroid testing is performed in vacuum, the microtoroid intrinsic Q may be increased beyond the current boundary. Higher quality factor in microtoroids will permit further research into other loss sources in microtoroids and increase the strong coupling between atoms and the cavity in cQED experiments. Other applications may be found in more efficient nonlinear effects of silica, due to the small mode volume and ultra-high Q of microtoroids.

6.4 Vacuum reflow system

A completely new and never-before demonstrated laser reflow and microtoroid testing system in vacuum was designed and built by the author. This system will drastically reduce or eliminate water adsorption onto the toroid surface after laser reflow, and maintain the toroid's pristine surface during fiber taper testing of the quality factor. As Gorodetsky proved, the initial Q of microcavities instantaneously after reflow is significantly higher than the steady-state Q measured in normal atmosphere after several hours, thought to be due to water content in the air. Laser annealing raises the temperature of silica above its melting point of $1,700^\circ\text{C}$, at which point the amorphous silica collapses into a torus shape due to surface tension. Annealing in vacuum at this high temperature will bake off water on the surface, and perhaps even water trapped inside the silica microdisk, reducing the absorption loss due to OH groups in the newly minted toroid cavity.

A diagram of the UHQ toroid in vacuum system is presented in Figure 6.1. A high power carbon dioxide (CO_2) gas laser generates a short pulse of infrared radiation at $10.6 \mu\text{m}$. The collimated laser pulse passes through several mirrors before the beam is focused down to a $200 \mu\text{m}$ diameter spot located $7''$ from the lens. The CO_2 laser pulse is focused down through the IR/visible beam combiner. This three-element optical system combines the laser beam line and imaging system beamline to simultaneously allow imaging and reflow of the microdisk. A silica microdisk, located in the exact center of the laser focus, is selectively reflowed by the invisible laser pulse into a

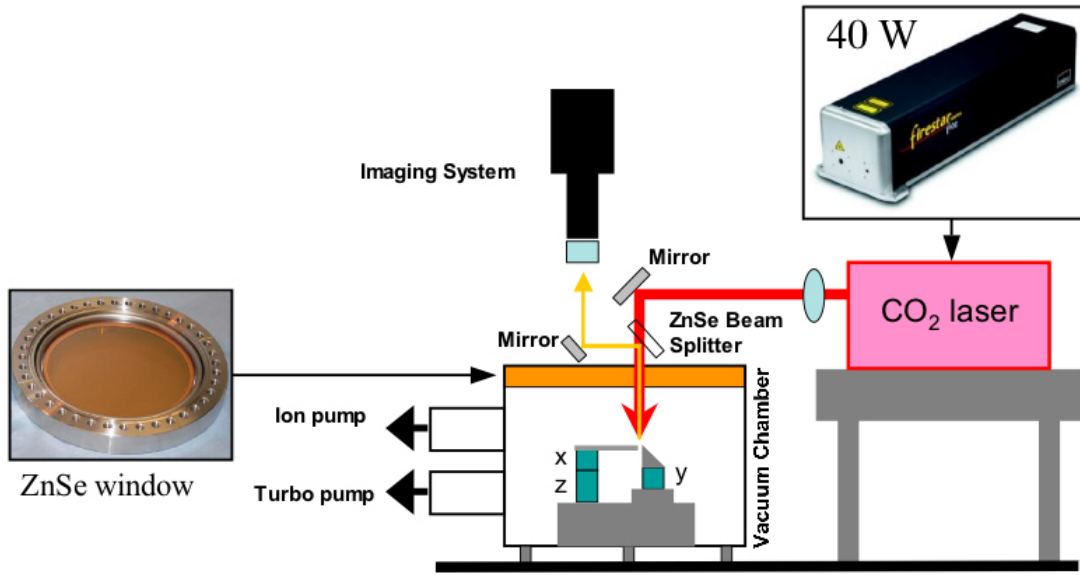


Figure 6.1. Schematic diagram of vacuum reflow concept. The CO₂ laser beam enters the vacuum chamber to reflow microtoroids, and the microtoroids are viewed with a microscope. Coupling is performed with nanopositioners in vacuum.

microtoroid.

The microtoroid is suspended on a silicon substrate, which can be precisely moved using a three-axis Attocube positioning system. After reflow, the microtoroid is translated into coupling with a single-mode fiber taper already resting in the vacuum on an aluminum fork. The combination stepping and piezo movement of the high-precision stages allow for critical coupling of the microtoroid to the tapered fiber. Finally, the intrinsic Q of the microtoroid is measured by cavity ringdown. This entire procedure occurs in high vacuum, at a pressure of 1×10^{-7} Torr. The following sections review the design considerations of the laser reflow and testing systems in vacuum.

6.4.1 Vacuum chamber

The vacuum chamber must be large enough to contain the nanopositioners, fiber taper, large ZnSe upper window, and allow connection of equipment used to maintain and measure the vacuum pressure. The author choose a cylindrical chamber with 8" diameter, 6" height, and a total of 7 vacuum ports. A turbo vacuum pump (Mini Task, Varian) evacuates the chamber from atmospheric pressure down to 1×10^{-5} Torr. However, the turbo pump is mechanical, and therefore causes significant vibrations that prevent stable taper coupling. So, a noble diode ion pump (Vacion Plus 55, Varian) is used to decrease the chamber pressure to 7×10^{-8} Torr. The vibrationless ion pump allows for

stable coupling between the toroid and the fiber taper. Two other ports are connected to low (7F, Televac) and high pressure (4A, Televac) vacuum pressure gauges. Also, several ports provide electrical feedthrough of the Attocube cables, and fiber feedthrough. The largest vacuum port connects to the 8" ZnSe window (Torr Scientific) that provides passage of the CO₂ laser beam and visible imaging beam into the chamber at low pressure. The stainless steel vacuum chamber is sourced from Nor-Cal Products Inc., and designed for operation at a pressure as low as 1×10^{-9} Torr.

6.4.2 CO₂ laser annealing

The microtoroid reflow step is the most crucial step in UHQ microtoroid fabrication. The microtoroid must be symmetrically illuminated by a CO₂ laser beam for symmetric reflow in order to show ultra-high Q . The laser beam spot at the microtoroid plane is a product of the laser source and all intermediate optics. A near diffraction-limited ($M^2 < 1.1$) collimated laser beam 2.5 mm in diameter is the output of a commercial high-power CO₂ laser (V40, Synrad). Only the highest quality infrared optics were chosen for the laser beamline. Two flat turning mirrors provide accurate beam alignment. A low-distortion ZnSe plano-convex lens with 7" focal length creates a circular beam spot in the focal plane, located inside the vacuum chamber. A third mirror directs the laser pulse down into the chamber, and through a ZnSe flat window that serves as the beam splitter. Finally, the laser beam passes through the 9 mm thick anti-reflection coated ZnSe vacuum window and a 1 mm thick uncoated ZnSe window that protects the ZnSe top window from contamination during laser reflow.

For laser reflow, the microdisk is imaged at lower resolution than used during testing. The distance between the beam combiner and the toroid resonator is large (100 mm), necessitating a long working distance lens objective that results in lower resolution (of order 5 μm). But, the image is sufficiently crisp to allow identification of the microdisk center and observation of the reflow process. The laser focus and microdisk center are aligned together with an alignment mark on the image screen.

The laser is carefully aligned to produce a symmetric and clean focus spot, verified by reflow of glass slides inside the vacuum chamber. The lens position is varied to find the optimum distance between the lens and the reflow plane, which may be different than the focal length. Initially, the silicon chip containing the microdisks to be reflowed was supported by an aluminum base. However, this base was eliminated after discovering that the reflow spot was asymmetric as a result of interference in the toroid plane caused by back reflection of laser light. Also, a thin metal plate bonded at 45° underneath the silicon chip is later added to eliminate a reflection from the aluminum taper holder base.

6.4.3 Microtoroid testing

A solid aluminum base with two towers provides the correct elevation and stable support for the separate taper fiber holder and silicon chip mount. Three Attocube nanopositioners (x,y,z) are stacked on top of one another. Attocube positioners were chosen for their combination of long-range motion (5 mm range), high-resolution (10 nm) piezo actuation, and stability in ultra-high vacuum (UHV). To prevent the laser reflow pulse from damaging or even breaking the fiber taper, the reflow spot is located several millimeters away from the fiber taper. After reflow, an array of up to seven microtoroids on chip is moved towards the fiber taper.

The fiber taper is pulled using a hydrogen flame and two motors until the single mode condition is verified by observing taper transmission dynamics in time. The taper is then transferred from the standard taper puller to an aluminum fork secured by epoxy. The taper is pulled to a smaller final length than normal to prevent transmission loss. The fork is only one inch wide and any portion of the fiber taper mode that encounters the epoxy will be scattered away. After being secured on the fork, the taper is transferred into the vacuum chamber and held over the silicon chip. Then, the top ZnSe window is secured and the chamber is evacuated.

After laser reflow in vacuum is completed, the beam combiner is removed, and a high-resolution objective replaces the long working distance lens to allow high resolution imaging (of order $2\ \mu\text{m}$) of the microtoroid. To achieve coupling between the toroid and taper, the toroid is first moved within ten microns of the taper in steps. Then, once a cavity resonance has been identified by tuning the single frequency 1550 nm diode laser, the toroid position is optimized into critical coupling with the taper by voltage control of the piezo. Piezo control provides ultra-smooth movement of the toroid and provides in stable coupling.

6.5 Vacuum reflow system assembly

The vacuum chamber is secured to an isolated optical table, and all the vacuum equipment is attached. With blank flanges covering unused ports, the vacuum system is tested for low pressure performance and baked out. Then, the CO_2 laser beam line is aligned carefully, ensuring that the beam is not clipped or distorted as it passes through the mirrors, lens, and windows. Figure 6.2 is a photograph of the CO_2 laser assembly and vacuum chamber.

The beam combiner was designed by the author to bring into co-linear propagation the laser and imaging beams. The combiner is cantilevered out over the ZnSe top window. A photograph of the beam combiner is given in Figure 6.3.

Finally, the vacuum interior is populated with the fiber taper holder (u-shaped fork), three nanopositioners, and the sample mount. A picture of the vacuum chamber inside, showing these components, is shown in Figure 6.4.

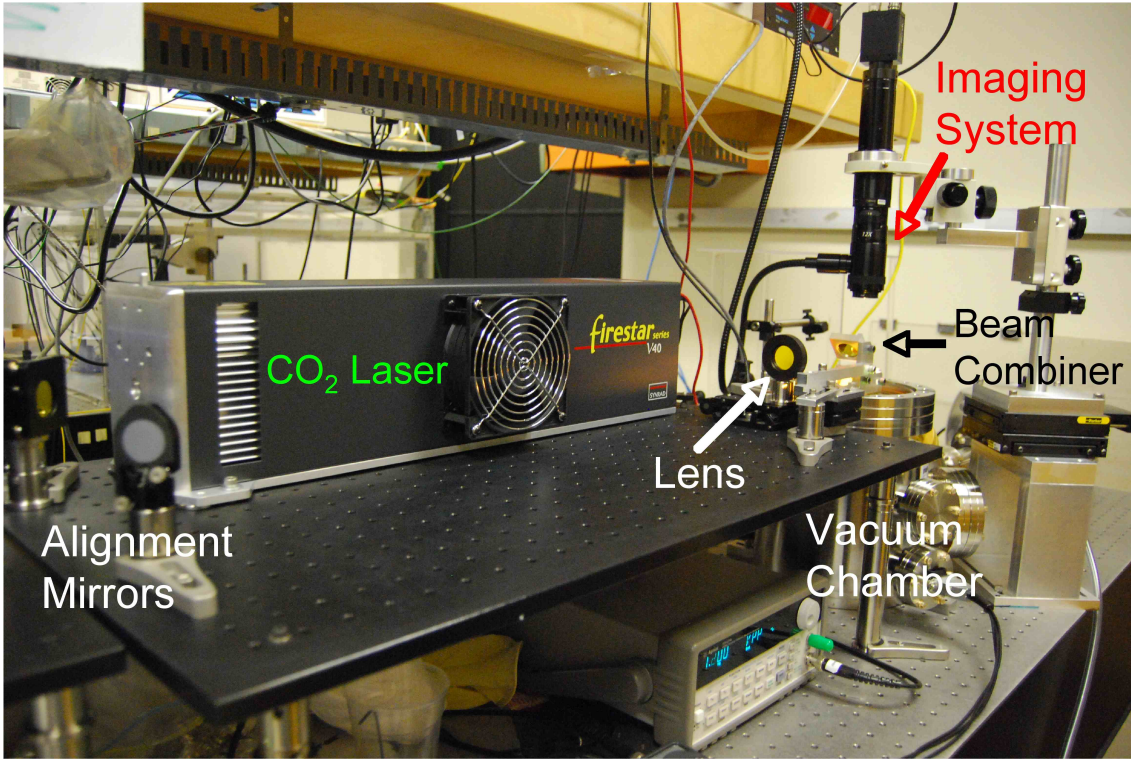


Figure 6.2. Image of CO₂ laser optics and vacuum chamber

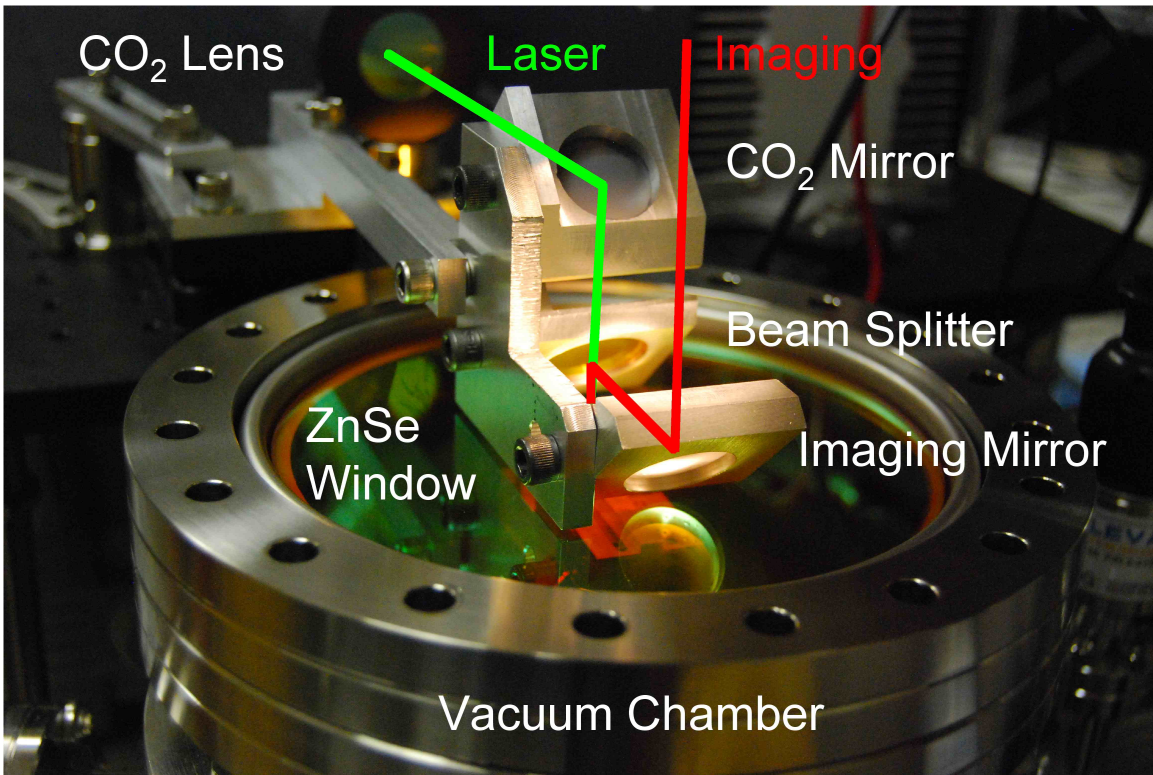


Figure 6.3. Image of laser and imaging beam combiner

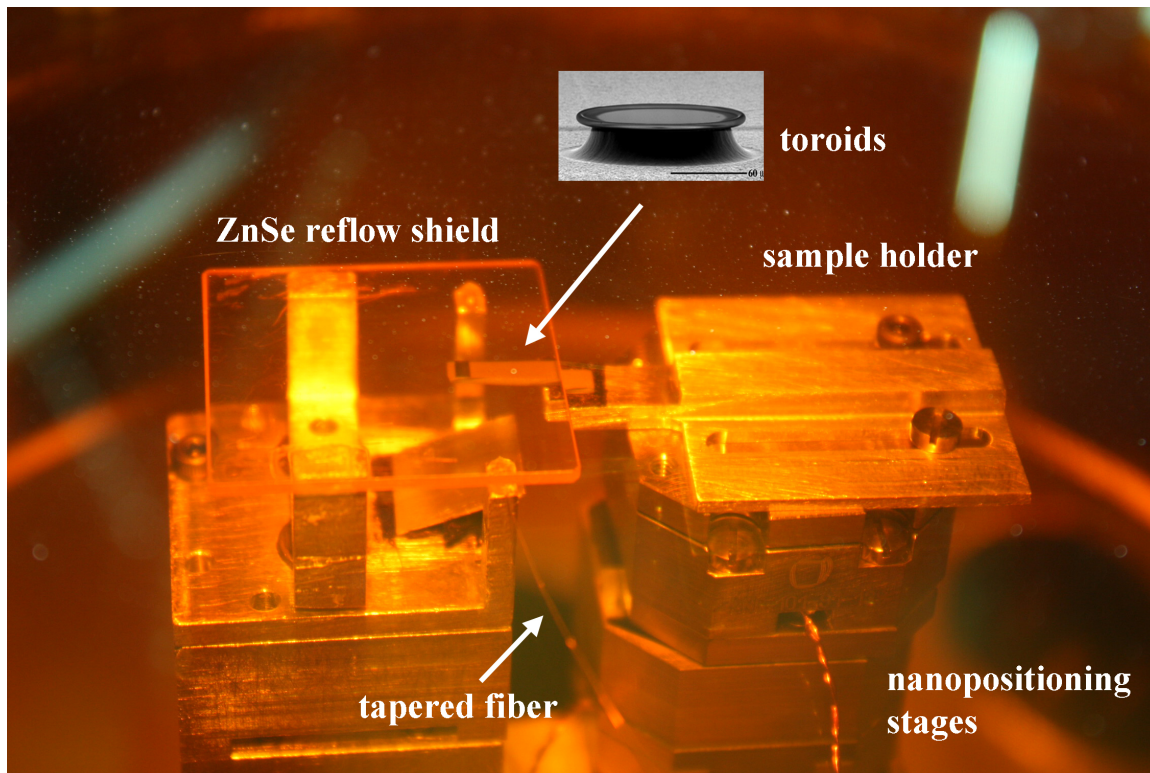


Figure 6.4. Image inside vacuum chamber of microtoroids, shown on a sample holder on nanopositioning stages, underneath a fiber taper. The top ZnSe window (not shown) is protected by a secondary ZnSe window (blast shield).

6.6 Microtoroid reflow and testing in vacuum

To achieve record Q of a microtoroid in vacuum, first the microdisk must have excellent quality. The microdisks were fabricated according to best practices in the Kavli Nanoscience Institute (KNI) at Caltech from 2 μm silicon dioxide layer on prime silicon. The silica layer was grown by wet deposition, which may leave behind lossy OH groups. In the future, silica grown by dry deposition will be tested. In addition to the use of advanced cleaning techniques during all stages of fabrication, the photolithography was done by a microelectronics industry-grade stepper and high resolution chrome mask. Also, best practices were employed during BOE wet etch and xenon difluoride dry etch used to define and isolate the silica microdisk on the silicon substrate. The 100 μm diameter microdisks show no imperfections or roughness, and provides an excellent preform for the silica microtoroid.

Next, the author aligned the CO_2 laser focal spot to the alignment mark by melting a glass slide. This alignment is performed in air, before the silicon chip with microtoroids is loaded into the vacuum chamber, because contamination occurs to anything close to the glass slide. This contamination may be due to impurities in the low quality microscope slide. In the future, higher quality glass may allow laser alignment under vacuum just prior to toroid reflow.

A single-mode optical fiber taper is pulled according to the standard taper fabrication method. As mentioned earlier, the taper length is half of the normal length to prevent leakage of the optical wave into the epoxy on the taper fork. The taper is epoxied to the taper fork, and transferred into the chamber while preserving greater than 90% transmission. The taper must have high transmission to prevent taper destruction in vacuum that can occur if the injected optical power exceeds 50 μW . While tapered fibers with micron scale diameters can carry milliwatts of optical power in air, the lack of air cooling in vacuum makes them more likely to burn. The fiber's input and output ends are routed through teflon inserts compressed by swagelock nuts, to form an UHV seal.

After the taper is placed into the chamber, the silicon chip with microdisks is fixed to its aluminum mount by SEM tape. The chip is cantilevered away from the mount, so that there is no surface immediately underneath the microdisks, preventing poor reflow quality due to reflection of unabsorbed CO_2 light. Figure 6.4 shows the silicon chip near the fiber taper inside the vacuum chamber.

The vacuum chamber is sealed with the large ZnSe window before the chamber's air is removed out by the turbo pump. After the pressure reaches 1×10^{-5} Torr, the noble diode ion pump is activated to further reduce the chamber pressure. After several hours of pumping, the turbo pump is turned off to eliminate vibrations. Then, the microdisks are moved into alignment centered on the alignment mark one by one. Each microdisk is reflowed with a single pulse from the CO_2 laser. A square pulse with 100 ms duration and 1 J of pulse energy is emitted from the laser, which is controlled by a function generator. Laser reflow of the silica microdisks produces microtoroids with

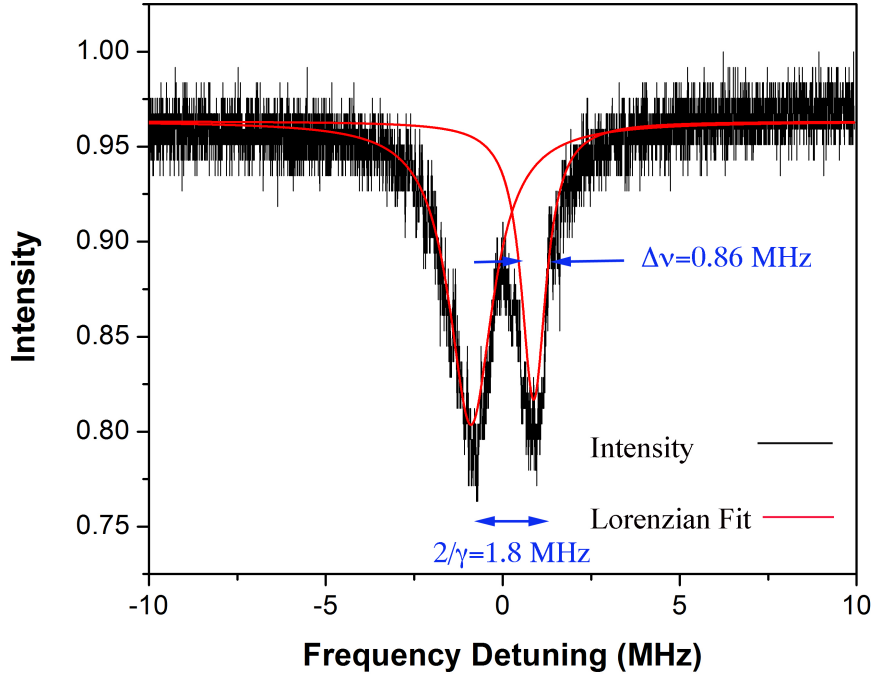


Figure 6.5. Plot of the taper transmission versus laser detuning frequency, showing a characteristic doublet mode of a microtoroid ($D = 55 \mu\text{m}$). The resonance lineshape of each mode (black) is fit to a Lorentzian (red). The sub MHz linewidth ($\Delta\nu$) of one resonance and the splitting frequency (γ^{-1}) are also marked.

$55 \mu\text{m}$ diameter.

The newly reflowed microtoroids are each analyzed in vacuum according to their cavity mode linewidths with a single frequency tunable diode laser. The highest Q measured to date in the vacuum reflow system is 2.1×10^8 , determined by resonance linewidth and cavity ringdown measurements. First, the linewidth of a whispering-gallery mode is recorded in the undercoupling regime, where intrinsic loss dominates. At an input power to the taper of only $2 \mu\text{W}$, no thermal broadening of the resonance is observed. Mode coupling due to internal scattering in the microtoroid causes previously degenerate counter-propagating modes to split in frequency. The WGM doublet resonance is shown in Figure 6.5, and is a plot of the taper transmission as a function of the diode laser detuning. The resonances are fit to a double peak Lorentzian lineshape, and the resonance linewidth is determined to be 7×10^{-15} m. Therefore, at a wavelength of 1548.1 nm , the intrinsic Q ($\lambda/\Delta\lambda$) is calculated by linewidth measurement to be 2.2×10^8 .

Since the diode laser linewidth ($\approx 300 \text{ kHz}$) is of the same order as the microtoroid's cavity frequency width (800 kHz), a more accurate measurement of the microtoroid's UHQ is performed

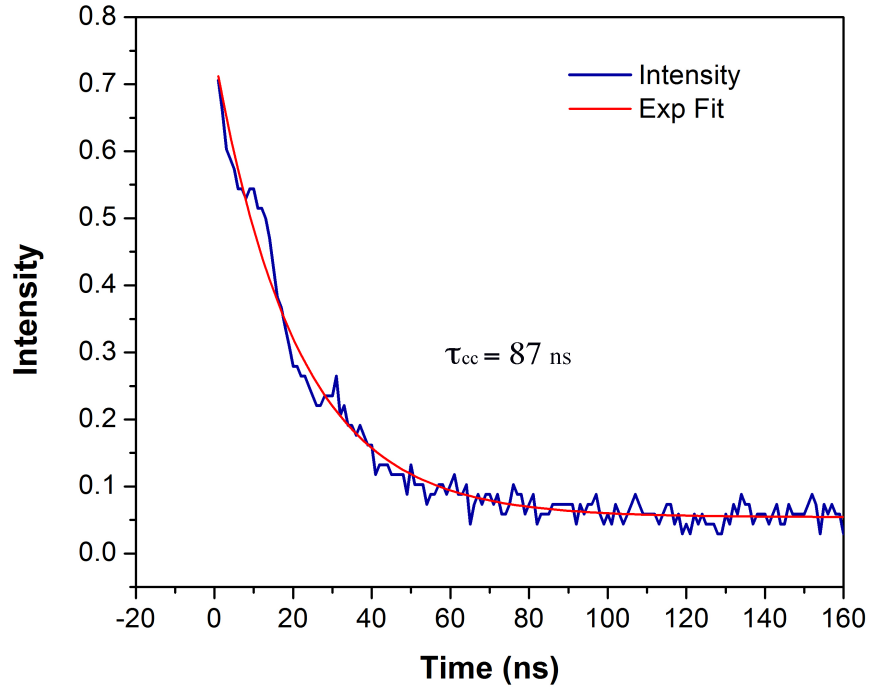


Figure 6.6. Plot showing a microtoroid cavity ringdown measurement in vacuum. The microtoroid laser cavity output is recorded after the input is gated off by a modulator. The intensity decay in time is fit to an exponential, and the cavity ringdown lifetime (τ_{cc}) at critical coupling is calculated.

by cavity ringdown. The cavity ringdown technique is described in **Chapter 2**. The taper and toroid are moved into critical coupling, exciting the toroid cavity with peak circulating power. At $t = 0$, the input laser field is switched to zero by an external phase modulator (8 ns fall time). Then, the taper transmission is recorded in time as the microtoroid cavity releases its stored energy with a measurable time constant, τ_{cc} . After an spike in transmitted power, the transmitted power decreases exponentially as shown in Figure 6.6.

The transmission is fitted to an exponential, whose time constant is the cavity lifetime $\tau_{cc} = 87$ ns. In order to accurately determine the intrinsic Q , the frequency separation of the split modes is need. The resonance linewidth measurement previously performed gives $\gamma^{-1} = 0.89$ MHz. With the critical coupling lifetime and splitting frequency now known, the intrinsic Q of this specific WGM is calculated to be 2.1×10^8 (see Equation (2.15)). The two separate methods for determining cavity Q produce nearly identical results for this vacuum annealed microtoroid.

6.7 Summary

In summary, the first toroid fabricated in the vacuum laser reflow and testing system has a maximum Q of 2.1×10^8 . In the future, the laser reflow process will be improved to yield higher Q , possibly record numbers. Also, the author will study the difference in intrinsic Q between toroids manufactured in vacuum from silica grown with wet versus dry deposition methods. The upper limits of quality factor will be studied.

If microtoroid loss can be reduced, new research applications may be found in nonlinear optics, cavity quantum electrodynamics, and narrow linewidth lasers. Microtoroids combine ultra-small mode volume with ultra-high Q whispering-gallery modes, making them excellent platforms for material research and sensing. In the future, this vacuum reflow and testing system may be used for CO₂ gas sensing.